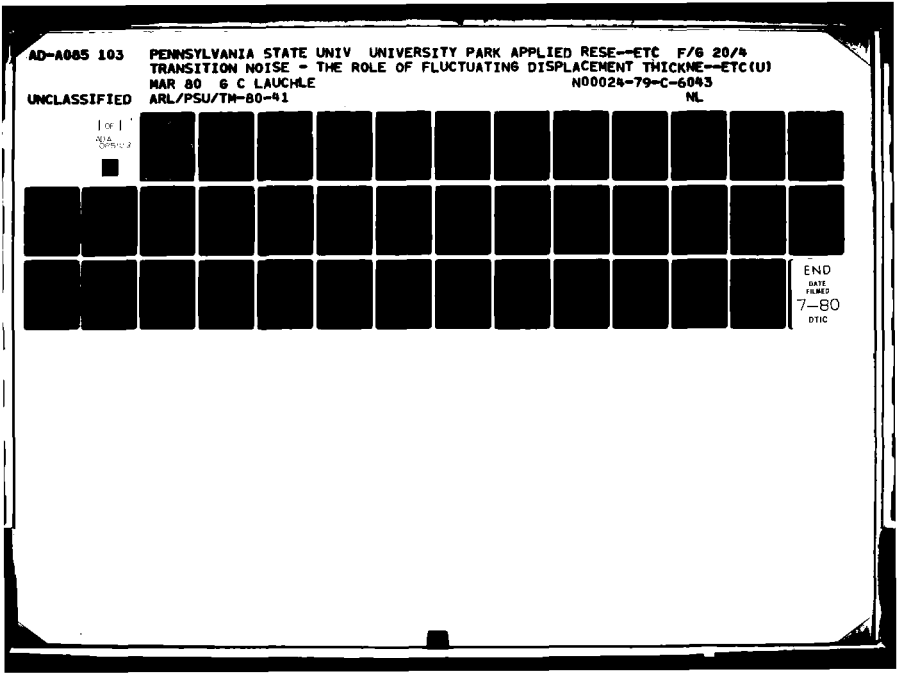
AD-A085 103
PENNSYLVANIA STATE UNIV UNIVERSITY PARK APPLIED RESE--ETC F/G 20/4
TRANSITION NOISE - THE ROLE OF FLUCTUATING DISPLACEMENT THICKNE--ETC(U)
MAR 80 G C LAUCHLE
N00024-79-C-6043
UNCLASSIFIED
ARL/PSU/TM-80-41
NL
1 OF 1
END
DATE FILMED
7-80
DTIC

JL.

12

LEVEL II

ADA085103

TRANSITION NOISE - THE ROLE OF FLUCTUATING DISPLACEMENT THICKNESS

G. C. Lauchle

Technical Memorandum
File No. TM 80-41
27 March 1980
Contract No. N00024-79-C-6043

Copy No. 37

The Pennsylvania State University
Institute for Science and Engineering
APPLIED RESEARCH LABORATORY
Post Office Box 30
State College, PA 16801

NAVY DEPARTMENT

NAVAL SEA SYSTEMS COMMAND

Approved for Public Release
Distribution Unlimited

UNCLASSIFIED
SECURITY CLASSIFICATION OF THIS PAGE (When Data Entered)

REPORT DOCUMENTATION PAGE	READ INSTRUCTIONS BEFORE COMPLETING FORM
1. REPORT NUMBER: TM 80-41	2. GOVT ACCESSION NO.: AD-A085 103
	3. RECIPIENT'S CATALOG NUMBER:
4. TITLE (and Subtitle): (6) TRANSITION NOISE - THE ROLE OF FLUCTUATING DISPLACEMENT THICKNESS,	5. TYPE OF REPORT & PERIOD COVERED: (9) Technical Memorandum
	6. PERFORMING ORG. REPORT NUMBER:
7. AUTHOR(s): (10) G. C. Lauchle	8. CONTRACT OR GRANT NUMBER(s): (15) N00024-79-C-6043
9. PERFORMING ORGANIZATION NAME AND ADDRESS: Applied Research Laboratory, P.O. Box 30, State College, PA 16801	10. PROGRAM ELEMENT, PROJECT, TASK AREA & WORK UNIT NUMBERS: (12) 39
11. CONTROLLING OFFICE NAME AND ADDRESS: Naval Sea Systems Command, Washington, DC 20362 (11)	12. REPORT DATE: 27 March 1980
	13. NUMBER OF PAGES: 32
14. MONITORING AGENCY NAME & ADDRESS (if different from Controlling Office): (14) ARL/PSU/TM-80-41	15. SECURITY CLASS. (of this report): UNCLASSIFIED
	15a. DECLASSIFICATION DOWNGRADING SCHEDULE:

16. DISTRIBUTION STATEMENT (of this Report)

Approved for Public Release. Distribution Unlimited.
Per NAVSEA - May 5, 1980.

17. DISTRIBUTION STATEMENT (of the abstract entered in Block 20, if different from Report)

18. SUPPLEMENTARY NOTES

19. KEY WORDS (Continue on reverse side if necessary and identify by block number)

boundary layer, displacement, fluctuating, turbulence

20. ABSTRACT (Continue on reverse side if necessary and identify by block number)

The role of the fluctuating wall shear stress on the noise generated by incompressible boundary-layer transition was recently analyzed ~~[C. C. Lauchle, J. Acoust. Soc. Am. 67, 158-168 (1980)]~~. The solutions of that analysis suggest that the shear stress mechanism generates hydrodynamic sound weakly in comparison say to the sound generated by a fully developed turbulent boundary layer flow. Because boundary-layer transition is a very unstable and non-steady flow, ~~we might~~ it is expected that other acoustic mechanisms exist.

DD FORM 1 JAN 73 1473 EDITION OF 1 NOV 65 IS OBSOLETE

UNCLASSIFIED 391007
SECURITY CLASSIFICATION OF THIS PAGE (When Data Entered)

In this paper, we examine one other; namely, that of the fluctuating boundary layer displacement thickness which is expected to occur as turbulent bursts are created and convected over the surface. The snslysis shows that a weak monopole sound source occurs, and at low subsonic flow velocities, this source generates significant acoustic energy. Comparisons of the theoretical predictions with available experimental data support this conclusion.

Subject: Transition Noise - The Role of Fluctuating Displacement Thickness

References: See page 22.

Abstract: The role of the fluctuating wall shear stress on the noise generated by incompressible boundary-layer transition was recently analyzed [G. C. Lauchle, J. Acoust. Soc. Am. 67, 158-168 (1980)]. The solutions of that analysis suggest that the shear stress mechanism generates hydrodynamic sound weakly in comparison say to the sound generated by a fully developed turbulent boundary layer flow. Because boundary-layer transition is a very unstable and non-steady flow, we might expect that other acoustic mechanisms exist. In this paper, we examine one other; namely, that of the fluctuating boundary layer displacement thickness which is expected to occur as turbulence bursts are created and convected over the surface. The analysis shows that a weak monopole sound source occurs, and at low subsonic flow velocities, this source generates significant acoustic energy. Comparisons of the theoretical predictions with available experimental data support this conclusion.

Acknowledgments: The author is grateful to Professor J. L. Lumley for an enlightening discussion regarding the possible role of fluctuating displacement thickness on boundary-layer noise. This work was supported by the U.S. Naval Sea Systems Command, Code 63R-31.

TABLE OF CONTENTS

LIST OF FIGURES

INTRODUCTION

This author has recently analyzed the role of the fluctuating wall shear stress on the radiated noise due to incompressible boundary-layer transition [1]. In the development of that solution, several types of sources were identified under the assumption of the boundary layer flow being confined to one side of an infinite rigid planar surface. Quadrupoles and octupoles resulted from the fluctuating Reynolds stresses and their images while a longitudinal dipole resulted from the shear stress fluctuations. Under the assumption of low Mach number flow, the dipole was considered to dominate and was hence analyzed in detail. Upon comparing predictions using the shear stress model for the noise with experimental data, rather poor agreement was achieved. Because the computed radiation efficiency was also found to be low, the discrepancy between theory and experiment was not unexpected. That is, the experiment was performed with a buoyant body that supports a substantial area of fully-developed turbulent flow which, based on the magnitude of relative radiation efficiencies, would be expected to dominate the noise spectrum.

Although controversy exists as to whether the transition zone is an important source of hydrodynamic noise, it appears that further analysis and experiment are required in order to resolve the issue. In the tutorial paper by Haddle and Skudrzyk [2], p. 149, the authors state, "...the region where turbulence starts is particularly unstable and intermittent, and must be expected to generate more sound than the rest of the unit." From experiments this author performed in The Garfield Thomas Water Tunnel [3], this statement was partially substantiated;

however, the theory of Ref. [1] does not predict any excessive noise over that of a turbulent boundary layer alone. Realizing that boundary-layer transition is a very complicated type of flow, the use of only one mechanism to describe its overall noise production is probably not justified. The shear stress mechanism certainly contributes, but it may not be the dominant one.

In this paper we will consider another type of mechanism; one that gives rise to monopole sound radiation. Its existence is established through a qualitative look into the physics of intermittent boundary-layer flow. It is well known from elementary boundary layer theory that the displacement thickness represents a distance from the wall through which the potential outer flow is displaced due to the presence of the boundary layer. In other words, it represents a mass flow deficit. Thus, if the displacement thickness is known to undergo fluctuations in time, then one can expect mass flow fluctuations near the surface. These fluctuations then act on the potential outer flow (acoustic medium) in much the same way as a vibrating surface acts on its surrounding medium. The normal velocity of the surface, which can be termed the piston velocity, defines a boundary condition with which the wave equation may be solved for the sound pressure. By constructing a model for the displacement thickness fluctuations that occur within the transition zone, an equivalent piston velocity is similarly defined. The wave equation is then solved by straightforward methods such as those used in the study of sound radiation from randomly vibrating structures.

The concept of a displacement effect is not new. It is discussed in some detail by Laufer, Ffowcs Williams, and Childress [4] in regards to

the noise generated by turbulent boundary layers. The idea was first proposed by Liepmann, but apparently was never published [4]. As long as the wave equation forms the basis for the modeling, the results derived from this approach should be equivalent to those derived from Lighthill's analogy. The main difference is that the unknown is now contained within the boundary condition and not within the source terms of Lighthill's equation.

The analysis presented in this paper is based on the displacement effect. The power spectrum and radiation efficiency are predicted using analytical techniques similar to those of Ref. [1]. To help in the verification of this theory, three examples will be presented in which experimental data exist.

I. ANALYSIS

Following Ref. [1], we consider the viscous flow of free-stream velocity u_0 over a flat plate. If a laminar boundary layer begins to form at the origin of our Cartesian coordinate system, and if the flow direction is in the x_1-direction, then the flow will ultimately become nonlinearly unstable at the downstream line $x_1 = x_0$ (see Fig. 1). There is then a short distance, Δx, over which turbulent "bursts" occur. Along $x_1 = x_0 + \Delta x$, the flow becomes fully turbulent while for $x_1 < x_0$, the flow is assumed completely laminar.

Within the source region, $x_0 \leq x_1 \leq x_0 + \Delta x$, the boundary layer intermittently changes from laminar to turbulent regimes. The bursts of turbulence usually grow as they convect downstream at some mean convection velocity, u_c. The locus of a typical burst forms a wedge of apex angle

2α, where we will assume Emmons' [5] result that $\alpha \simeq 9.6°$. Now, at any arbitrary location within the source region, there are going to be instants of time when the boundary-layer flow is laminar while at other instants it will be turbulent. The intermittency factor, $\gamma(x_1)$, is a measure of the percentage of time that the boundary layer is turbulent. Through very carefully performed experiments on a flat plate, Dhawan and Narasimha [6] showed that at x_1 where $0 < \gamma(x_1) < 1$, the mean value of boundary layer displacement thickness is given simply by:

$$<\delta^*> = (1 - \gamma)\ \delta_L^* + \gamma\delta_T^* \quad , \tag{1}$$

where subscript L stands for the laminar flow value and T stands for the corresponding turbulent flow value. We will assume for the laminar flow regimes a Blausius velocity profile; thus, from Schlichting [7]:

$$\delta_L^* = 1.7208\ \frac{\nu}{u_0}\ Re_{x_1}^{1/2} \quad , \tag{2}$$

where ν is the kinematic viscosity of the fluid and Re_{x_1} is the local value of length Reynolds number $(u_0\ x_1/\nu)$. Within the turbulent bursts we will assume a one-seventh power law for the velocity profile, from which [7]:

$$\delta_T^* = 0.04625\ x_1\ Re_{x_1}^{-1/5} \quad . \tag{3}$$

Both Eq. (2) and Eq. (3) were developed under the assumption of a zero pressure gradient, but they may be used with reasonable confidence in flows with mild favorable pressure gradients.

The temporal variation of δ^* through the transition zone is the most important ingredient in the development of the present acoustic theory. No known measurements are available; therefore, we must propose a mathematical model based upon physical intuition. This was the approach used to model the fluctuating wall shear stress in the previous analysis [1]. Realizing that δ^* cannot instantaneously change from a laminar value [Eq. (2)] to a turbulent value [Eq. (3)], we must introduce a time constant, t_i, which mimics the time required for δ^* to change from δ_L^* to δ_T^* (rise time) or visa versa (fall time). For the purposes of the current analysis we will assume the rise time equals the fall time and that during the rise and fall periods, δ^* obeys an exponential dependence with time. Thus, we propose that at a point:

$$\delta^*(t) = [1 - \tilde{I}(t)]\ \delta_L^* + \tilde{I}(t)\ \delta_T^* \quad , \tag{4}$$

where $\tilde{I}(t)$ is a random indicator function as shown in Fig. 2(a).

Following Laufer, et.al. [4], the linearized boundary condition on the acoustic field is

$$v_n = \left(\frac{\partial \phi}{\partial x_2}\right)_{x_2 = 0} = \frac{\partial \delta^*}{\partial t} \quad , \tag{5}$$

where ϕ is the velocity potential of the sound field. From Eq. (4), Eq. (5) becomes

$$v_n = \Delta\delta^*\ \dot{\tilde{I}}(t) \quad , \tag{6}$$

where $\Delta\delta^* \equiv \delta_T^* - \delta_L^*$ and $\dot{\tilde{I}} = \partial\tilde{I}/\partial t$ which is depicted in Fig. 2(b). The velocity, v_n is the equivalent "piston velocity" of the surface due to fluctuations in the boundary layer displacement thickness. The acoustic problem now becomes one of a flexible plane surface of pre-scribed normal velocity, v_n. The solution for the sound field is well known. Crighton [8] gives a concise derivation, finding:

$$p(r,t) = \frac{\rho}{4\pi r}\frac{\partial}{\partial t}\iint_S v_n\left[\underline{\eta},\ t - \frac{|\underline{x} - \underline{\eta}|}{c}\right] d\underline{\eta} \quad , \tag{7}$$

where p is the acoustic pressure, ρ is the fluid mass density, $r = |\underline{x}|$, c is the sound velocity, and S is the area covered by the sources. Equation (7) shows no angular dependence; hence, the displacement effect creates monopole-type sound radiation. This equation can be simplified somewhat. Consider for the surface a typical length scale, W (Fig. 1), and for the transition zone, length and velocity scales Δx and u_c, respectively. Then, Crighton shows that

$$p(r,t) \simeq \frac{\rho}{4\pi r}\frac{\partial}{\partial t}\iint_S v_n(\underline{\eta},\ t - r/c)\, d\underline{\eta} \tag{8}$$

if and only if $W/c << \Delta x/u_c$. In this simplification, the integral may be interpreted as the total instantaneous rate of mass outflow created by the surface.

Substituting for v_n, Eq. (8) takes on the form:

$$p(r,t) \simeq \frac{\rho}{4\pi r}\frac{\partial}{\partial t}\int_0^{\Delta x}\int_{-\infty}^{\infty} \Lambda\delta^*(\eta_1)\dot{\tilde{I}}(\eta_1,\eta_3,\ t - r/c)\, d\eta_1\, d\eta_3 \quad , \tag{9}$$

where the origin of our coordinate system has been displaced x_0 units downstream.

A. Power Spectral Density

By definition, the power spectral density function may be derived from the Fourier transform of the autocorrelation function of the radiated acoustic pressure, i.e.,

$$G(r,f) = 2 \int_{-\infty}^{\infty} \langle p(r,t)\ p(r,t+\tau) \rangle\ e^{i\omega\tau}\ d\tau \quad , \tag{10}$$

where $\omega = 2\pi f$ which is the radian frequency and τ is the delay time associated with the correlation function. We would like to simplify Eq. (9) one step farther by making a parallel flow assumption over the source region. Thus, $\Delta\delta^*(\eta_1)$ is considered independent of η_1 which is certainly plausable when Δx is small. The term $\Delta\delta^*$ may be brought outside the integrals and evaluated at some average value of x_1, e.g., $\bar{x}_1 = x_0 + \Delta x/2$.

Equation (10) is now of the form:

$$G(r,f) \simeq \frac{\rho^2 (\Delta\delta^*)^2\ \omega^2}{8\pi^2\ r^2} \iiiint \langle \dot{I}(\eta_1,\eta_3,t - r/c)$$

$$\cdot\ \dot{I}(\eta_1 + \xi_1,\ \eta_3 + \xi_3,\ t - r/c + \tau) \rangle e^{i\omega\tau}\ d\eta_1\ d\eta_3\ d\xi_1\ d\xi_3\ d\tau,$$

where the ω^2 arises from the Fourier transform of the second time derivative of the space/time correlation function of $\dot{I}$. As in Ref. [1], we assume $\dot{I}$ to be stationary in time, homogeneous in x_3, and non-homogeneous in x_1. Then,

$$G(r,f) \simeq \frac{\rho^2 (\Delta\delta^*)^2 \omega^2}{8\pi^2 r^2} \iiiiii \langle \dot{I}(\eta_1,0,0) \cdot \dot{I}(\eta_1 + \xi_1, \xi_3, \tau) \rangle e^{i\omega\tau} \, d\eta_1 \, d\eta_3 \, d\xi_1 \, d\xi_3 \, d\tau \quad . \tag{11}$$

A very useful theorem, given by Stratonovich [9], allows us to rewrite Eq. (11) in terms of the correlation function for a random sequence of delta functions, $\dot{I}(t)$ [Fig. 3(a)] and a "frequency depression factor," $|J(i\omega)|^2$. The quantity $J(i\omega)$ is simply the Fourier transform of an individual pulse shape of Fig. 2(b). Using this theorem, Eq. (11) is identical to:

$$G(r,f) \simeq \frac{\rho^2 (\Delta\delta^*)^2 \omega^2}{8\pi^2 r^2} |J(i\omega)|^2 \iiiiii \langle \dot{I}\dot{I}' \rangle e^{i\omega\tau} \, d\underline{\eta} \, d\underline{\xi} \, d\tau \quad ,$$

where $\langle \dot{I}\dot{I}' \rangle$ is shorthand notation for the space/time correlation function. Again noting [1] that $\langle \dot{I}\dot{I}' \rangle = - \partial^2 \langle II' \rangle / \partial\tau^2$, Eq. (11) becomes:

$$G(r,f) \simeq \frac{\rho^2 (\Delta\delta^*)^2 \omega^4}{8\pi^2 r^2} |J(i\omega)|^2 \iiiiii \langle I(\eta_1,0,0) \cdot I(\eta_1 + \xi_1, \xi_3, \tau) \rangle e^{i\omega\tau} \, d\eta_1 \, d\eta_3 \, d\xi_1 \, d\xi_3 \, d\tau \quad , \tag{12}$$

where I(t) is the "ideal" indicator function of Fig. 3(b). The frequency depression factor is easily calculated:

$$J(i\omega) = \frac{1}{2} V_0 \int_{-\infty}^{\infty} e^{-|t|/t_i} e^{i\omega t}\, dt = V_0 \int_{0}^{\infty} e^{-t/t_i} e^{i\omega t}\, dt \quad . \tag{13}$$

The constant V_0 is determined from the condition [9] that $J(0) = 1$. We find $V_0 = t_i^{-1}$, from which Eq. (13) becomes:

$$J(i\omega) = (1 - i\omega t_i)^{-1} \quad ,$$

and

$$|J(i\omega)|^2 = [1 + (\omega t_i)^2]^{-1} \quad . \tag{14}$$

The integrals of Eq. (12) are now identical to those treated in Eq. (23) of Ref. [1]. We will not repeat the details here, but point out that <II'> was assumed separable, i.e.,

$$\langle II' \rangle = R_1(\eta_1, \xi_1, \tau)\, R_2(\eta_1, \xi_3) \quad , \tag{15}$$

where

$$\int_{-\infty}^{\infty} R_2(\eta_1, \xi_3)\, d\xi_3 \simeq 3\, \eta_1 \tan\alpha \quad , \tag{16}$$

and

$$R_1(\eta_1, \xi_1, \tau) \simeq \gamma(\eta_1) \exp(-\alpha^* |\xi_1|) \exp(-2N|\tau - \xi_1/u_c|) \tag{17}$$

with

$$\alpha^* \simeq (1 + 83.35\, z^8)/\Delta x \tag{18}$$

$$\gamma(z) \simeq 1 - e^{-4.185\, z^2} \tag{19}$$

$$N(z) \simeq 1.272\ (u_0/\Delta x)ze^{-4.185\ z^2} \tag{20}$$

and $$z = \eta_1/\Delta x \quad . \tag{21}$$

The distributions for the intermittency factor and burst frequency given in Eqs. (19) and (20), respectively are taken from Farabee, et. al. [10].

The power spectral density of the far-field acoustic pressure radiated per unit spanwise width of boundary-layer transition becomes:

$$\frac{\partial G(r,f)}{\partial x_3} \simeq \frac{\rho^2(\Delta\delta^*)^2\ u_0\ u_c^2}{8\pi^2\ r^2}\ F^*(k_c\Delta x,\ \alpha^*\Delta x,\ u_c t_i/\Delta x,\ u_c/u_0) \quad , \tag{22}$$

where $$F^* = \frac{(k_c\Delta x)^2\ F(k_c\Delta x,\ \alpha^*\Delta x,\ u_c/u_0)}{[1 + (k_c\Delta x)^2(u_c t_i/\Delta x)^2]} \quad , \tag{23}$$

$$F(k_c\Delta x,\alpha^*\Delta x,u_c/u_0) = (k_c\Delta x)^2 \int_0^1 \frac{1.272z^2(1-e^{-4.185z^2})e^{-4.185z^2}}{\left(6.472\left(\frac{u_0}{u_c}\right)^2 z^2e^{-8.37z^2}+(k_c\Delta x)^2\right)[(\alpha^*\Delta x)^2+(k_c\Delta x)^2]^{1/2}}$$

$$\cdot \left\{ \frac{2\alpha^*\Delta x}{[(\alpha^*\Delta x)^2+(k_c\Delta x)^2]^{1/2}} - e^{-\alpha^*\Delta xz}\sin(k_c\Delta xz-\phi)+e^{-\alpha^*\Delta x(1-z)}\sin[k_c\Delta x(1-z)-\phi] \right\} dz, \tag{24}$$

with $$\phi = \tan^{-1}\ (\alpha^*\Delta x/k_c\Delta x) \quad , \quad \text{and } k_c = \omega/u_c \quad .$$

Equation (23) has been integrated numerically by Simpson's rule. Typical results of this computation are presented in Figs. 4 and 5. It is seen from these figures that the magnitude of the high-frequency portion of the spectrum depends significantly on the value of the nondimensional rise time, $u_c t_i/\Delta x$. At very low values of $k_c \Delta x$, the spectral levels rise at 12 dB/octave and are essentially independent of $u_c t_i/\Delta x$. For $k_c \Delta x \gg 1$, the spectral levels roll off at 6 dB/octave. The frequency of the peak in the spectrum depends upon $u_c t_i/\Delta x$.

As noted in Figs. 4 and 5, the selected range for the nondimensional rise time is between 0.05 and 1.35. This range was established through the following dimensional reasoning. We expect that t_i scales with the length $\Delta\delta^*$ and with the velocities very near and normal to the surface; these velocities scale with the friction velocity, u_*. Thus, $t_i \sim \Delta\delta^*/u_*$. Letting $u_* \simeq u_0/30$ and $u_c \simeq 0.7\, u_0$, we conclude that

$$\frac{u_c t_i}{\Delta x} \sim 20 \frac{\Delta\delta^*}{\Delta x} \quad . \tag{25}$$

For typical values of $\Delta\delta^*$ and Δx as will be discussed in SECTION II, the above relationship suggests that $0.05 \leq u_c t_i/\Delta x \leq 1.35$.

B. Radiation Efficiency

If we denote the right-hand side of Eq. (22) by $\langle p_0^2 \rangle$, then the power radiated per unit spanwise width is given by:

$$N_a = \int_0^\infty \frac{\langle p_0^2 \rangle}{\rho c}\, d\omega \int_0^{2\pi} d\theta \int_0^\pi r^2 \sin\theta\, d\theta \quad . \tag{26}$$

substituting for $\langle p_0^2 \rangle$, we find:

$$N_a \simeq \frac{\rho(\Delta\delta^*)^2 u_0 u_c^3 \overline{F^*}}{2\pi c \Delta x} \quad , \tag{27}$$

where

$$\overline{F^*} = \int_0^\infty F^* \, d(k_c \Delta x) \quad . \tag{28}$$

The numerical value of $\overline{F^*}$ depends upon $u_c t_i/\Delta x$, where typical values are tabulated on Figs. 4 and 5. The radiation efficiency is defined as the ratio of acoustic power to hydrodynamic power generated by the source region. It was shown by Lauchle [1] that the hydrodynamic power for transitional flow is given by:

$$N_h \simeq 0.572 \, u_0 \, \Delta x \, \sigma \tag{29}$$

where $\sigma \equiv \tau_T(x_0) - \tau_L(x_0)$ which is the difference between the turbulent and laminar values of wall shear stress at the beginning of intermittent flow. Dividing Eq. (28) by Eq. (29), the transition zone radiation efficiency results:

$$\eta_{tr} \simeq 0.278 \frac{\rho u_c^3}{c\sigma} \left(\frac{\Delta\delta^*}{\Delta x}\right)^2 \overline{F^*} \quad . \tag{30}$$

Noting that $\Delta\delta^*/\Delta x$ is only weakly dependent on u_0 and that $\sigma \sim \rho u_0^2$, $\eta_{tr} \sim u_0/c$ which is to be expected for a monopole source.

In analyzing the role of shear stress fluctuations on transition noise [1], the computed radiation efficiency was compared with that of a fully developed turbulent boundary layer flow [11]. Repeating that comparison here, for the case of a fluctuating displacement thickness mechanism, we find:

$$\frac{\eta_{tr}}{\eta_{TBL}} \simeq 1.48 \left[\frac{\rho c\ \Delta\delta^*}{\Delta x}\right]^2 \frac{u_c^3\ \overline{F^*}}{\sigma\ \tau_T\ u_0} \quad , \tag{31}$$

where $\eta_{TBL} \simeq 0.188\ \tau_T\ u_0/\rho c^3$. Noting that $u_c \sim u_0$, and that $\sigma\ \tau_T \sim (\rho\ u_0^2)^2$, Eq. (31) shows that $\eta_{tr} \sim \eta_{TBL}/M^2$, where M is the free-stream Mach number. Through use of an emperical relation for Δx derived by Chen and Thyson [12], i.e.,

$$\Delta x \simeq 60\ x_0\ Re_{x_0}^{-1/3} \quad , \tag{32}$$

where Re_{x_0} is the transition point Reynolds number, and through use of Eqs. (2) and (3), it is easy to show that

$$\Delta\delta^*/\Delta x \simeq 7.708 \times 10^{-4}\ Re_{x_0}^{2/15} - 2.868 \times 10^{-2}\ Re_{x_0}^{-1/2} \quad . \tag{33}$$

Also, from Ref. [1],

$$\sigma\ \tau_T \simeq \left[0.0288\ \rho\ u_0^2\ Re_{x_0}^{-1/5}\right]^2 \left[1 - 11.53\ Re_{x_0}^{-3/10}\right] \quad . \tag{34}$$

Thus, η_{tr}/η_{TBL} depends only upon Re_{x_0}, M, and $u_c t_i/\Delta x$. Figure 6 shows the dependence of η_{tr}/η_{TBL} on M for a range of rise times and with $Re_{x_0} = 4 \times 10^6$ and $u_c = 0.8\ u_0$.

Some caution should be exercised when interpreting Fig. 6. The ratio of radiation efficiencies presented here assumes equal source areas. In practice, say for a body of revolution moving through water, the area of transition is $\Delta x W$ while the area of fully-developed turbulent flow is of the same order as the body surface area, A_b. Clearly, $A_b >> \Delta x W$ which means that a measured radiated noise spectrum may certainly contain significant contributions from the fully-developed turbulent flow.

II. EXAMPLES

By way of numerical examples, we will consider those cases in which flow noise was measured experimentally under anechoic or near-anechoic conditions. It is pointed out from the outset that for each of these examples, the experimentalists' goal was to measure the overall flow noise of the vehicle or fixture at different points in space. We therefore select those measurement points which, based on our physical insight, would appear to be most influenced by the noise generated by the transition zone. It is further pointed out that many of the hydrodynamic parameters that characterize the transition zone flow are not available for the examples discussed below. We have therefore estimated them using theoretical considerations. The most significant unknown is the rise time, t_i. Because there are no definitive measurements of this time constant, we have elected to use the dimensional analysis that led to Eq. (25).

A. Case 1: Flat Plate in Air

DeMetz and Casarella [13] performed extensive measurements of the fluctuating pressures that occur within the transition region of a large flat plate operating in an anechoic wind tunnel. Of their data, we select a condition where the microphone was located within the laminar boundary layer so that its response would be due only to the noise generated by the downstream unsteady flow. A spectrum of this noise is presented in Fig. B-3 of Ref. [13]. Here, $Re_{x_0} = 7.5 \times 10^6$ and the measurement took place at $Re_{x_1} = 4.758 \times 10^6$. Based on the difference of these two Reynolds numbers, r can be estimated to be 1.55 m. The width of the plate, W, is 2.44 m, which is multiplied by Eq. (22) in order to obtain the radiated noise due to the entire width of transitional flow. Now, the total plate length is 4.34 m and $x_0 = 4.26$ m; therefore $\Delta x \simeq 76$ mm. In other words, transition has occurred right before the trailing edge and the data should therefore be uncontaminated by any noise due to fully-developed turbulent flow [Eq. (32) predicts $\Delta x > 76$ mm].

Assuming $u_c/u_0 = 0.8$, the comparison of our prediction with the experimental spectrum is shown in Fig. 7. DeMetz, et. al. [13] attribute the high energy levels between 5 and 10 kHz as being due to pinhole microphone cavity resonance and plate vibration. Aside from this band, the data compare quite favorably with the present model using $u_c t_1/\Delta x = 0.15$. Also shown on Fig. 7 is a prediction for the shear stress contribution to the transition zone noise [1]. Clearly, the fluctuating displacement thickness mechanism appears to dominate.

B. Case 2: Buoyant Body in Water

Haddle and Skudrzyk [2] present flow noise spectra measured both on and far away from a buoyantly-propelled axisymmetric body with a hemispherical nose. Because the terminal velocity is quite high (30-37 knots), it is assumed that transition occurs on the 0.48 m diameter body before the laminar separation point. We assume transition occurs at the minimum pressure point which is predicted to be at $x_0 \simeq 0.32$ m [14]. Thus, for the 37 knot condition, $Re_{x_0} \simeq 6.27 \times 10^6$ which assumes 21°C fresh water. The length W is calculated from the circumference of the body at x_0. Hydrophone no. 7 which is located at a 45° arc from the stagnation point is selected for the first comparison. The estimated point of transition is 0.13 m downstream from this hydrophone (thus, r = 0.13 m).

The spectrum measured by hydrophone no. 7 is presented in Fig. 17 of Ref. [2]. We repeat it here in Fig. 8 along with the transition zone noise predictions for both mechanisms. Again rather good agreement is achieved for the noise mechanism addressed in this paper. It is noted, however, that the experimental spectrum rolls off slightly faster than the predictions. This may be due to a water-borne diffraction loss which was discussed in some detail by Lauchle [3].

Haddle and Skudrzyk also measured the far-field noise of the buoyant unit with a distant hydrophone array, e.g., Fig. 19 of Ref. [2]. The reference distance is the radius of a sphere whose area is the same as the area of the vehicle, i.e., r = 0.73 m. This run was performed at 30 knots, hence, $Re_{x_0} \simeq 4.97 \times 10^6$. A comparison of our predictions with the experimental spectrum is shown in Fig. 9. The shear stress contribution [1] is not shown because its directivity function would predict a null at

the beam aspect angle. It is of interest to note that $\Delta\delta^*$ is calculated to be 0.43 mm for these experiments and Δx was estimated to be 61 mm. Equation (25) then suggests that $u_c t_i/\Delta x \simeq 0.14$ which agrees to within a factor of three of that value used for the prediction which fits the data the best.

III. CONCLUSIONS

In this paper we have analyzed the role of a fluctuating displacement thickness on the noise generated by incompressible boundary-layer transition. In essence, the analytical methods parallel those of an earlier analysis in which the role of a fluctuating shear stress was addressed [1]. Based on numerical calculations of the power spectral density and on the relative magnitudes of the radiation efficiency, the mechanism treated in the present paper is found to be much more productive as a noise source than is the shear stress mechanism. The fluctuating displacement thickness effect gives rise to a monopole-type of sound radiation. The spectrum of the radiated noise was found to rise at 12 dB/octave, level off, and then fall off at 6 dB/octave.

The frequency at which the spectrum peaks is not easily defined because it depends upon a characteristic time, t_i, associated with the growth of the turbulent boundary layer in a turbulent burst. This time models the time required for the laminar value of the boundary layer displacement thickness to change to a turbulent value and visa versa. The way in which we incorporated t_i into the noise analysis is heuristic. We assumed that the displacement thickness grows from a laminar value to a turbulent value according to an exponential time variation and that the

process is symmetrical. There is no experimental evidence that this is true (or for that matter, any other functional form.) Based on the comparisons of this theory with experimental data, particularly those of Case 1, it appears that these assumptions may be realistic.

A basic problem to be resolved deals with the measurement of t_i. According to Laufer, et. al. [4], $\delta^*(t)$ can, in principle, be measured in a laboratory frame of reference by performing simultaneous measurements of the fluctuating velocity and pressure and their correlation through the boundary layer. One then couples these data with a first order partial differential equation for δ^* derived by integrating the non-steady continuity equation across the boundary layer. If this procedure can be demonstrated, then it is conceivable that t_i can also be measured. Such measurements, to this author's knowledge, have never been carried out. Perhaps the findings presented in this paper may provide the impetus required for future experimental investigations of this type.

REFERENCES

1. G. C. Lauchle, "On the Radiated Noise due to Boundary-Layer Transition," J. Acoust. Soc. Am. 67, 158-168 (1980).

2. G. P. Haddle and E. J. Skudrzyk, "The Physics of Flow Noise," J. Acoust. Soc. Am. 46, 130-157 (1969).

3. G. C. Lauchle, "Noise Generated by Axisymmetric Turbulent Boundary-Layer Flow," J. Acoust. Soc. Am. 61, 694-702 (1977).

4. J. Laufer, J. E. Ffowcs Williams, and S. Childress, "Mechanism of Noise Generation in the Turbulent Boundary Layer," AGARDograph 90 (1964).

5. H. W. Emmons, "The Laminar-Turbulent Transition in a Boundary Layer - Part I," J. Aero. Sci. 18, 490-498 (1951).

6. S. Dhawan and R. Narasimha, "Some Properties of Boundary Layer Flow During the Transition from Laminar to Turbulent Motion," J. Fluid Mech. 3, 418-436 (1958).

7. H. Schlichting, Boundary-Layer Theory (McGraw Hill, New York, 1968), 6th ed., pp. 130, 599.

8. D. G. Crighton, "Basic Principles of Aerodynamic Noise Generation," Prog. Aerosp. Sci. 16, 31-96 (1975).

9. R. L. Stratonovich, Topics in the Theory of Random Noise, Volume I (Gordon Breach Science Publ., New York, 1963), p. 157.

10. T. M. Farabee, M. J. Casarella, and F. C. DeMetz, "Source Distribution of Turbulent Bursts During Natural Transition," David W. Taylor Naval Ship Research and Development Center Report SAD-89E-1942, August 1974.

11. C. K. W. Tam, "Intensity, Spectrum, and Directivity of Turbulent Boundary Layer Noise," J. Acoust. Soc. Am. 57, 24-34 (1975).

12. K. K. Chen and N. A. Thyson, "Extension of Emmons' Spot Theory to Flows on Blunt Bodies, AIAA J. 9, 821-825 (1971).

13. F. C. DeMetz and M. J. Casarella, "An Experimental Study of the Intermittent Properties of the Boundary Layer Pressure Field During Transition on a Flat Plate," David W. Taylor Naval Ship Research and Development Center Report 4140, AD-775-299 (November 1973).

14. These distances are arc lengths originating at the stagnation point.

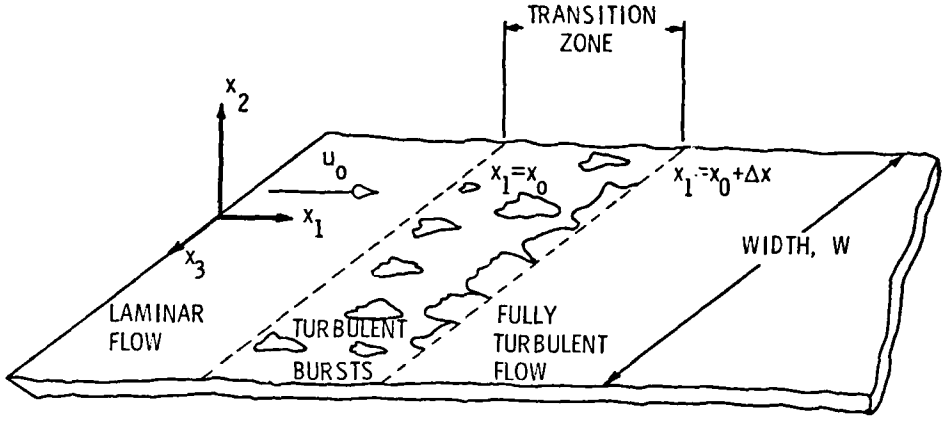

Fig. 1. Schematic representation of the transition from laminar-to-turbulent flow on a flat plate.

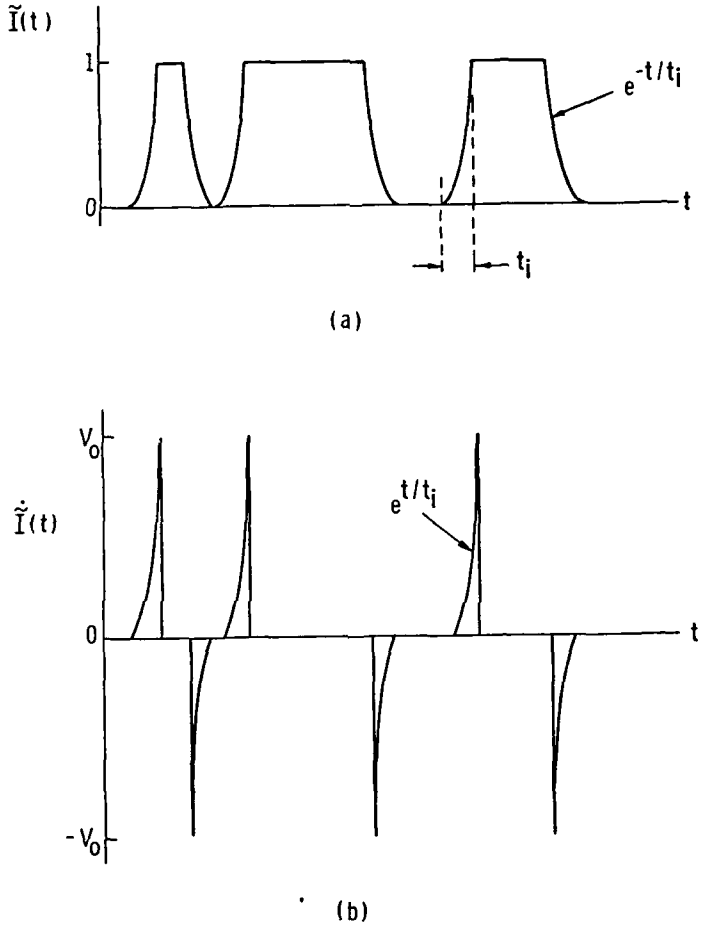

Fig. 2. The indicator function (a) and its first time derivative (b) which is used to model the random variation in displacement thickness during transition.

27 March 1980
GCL/pjk

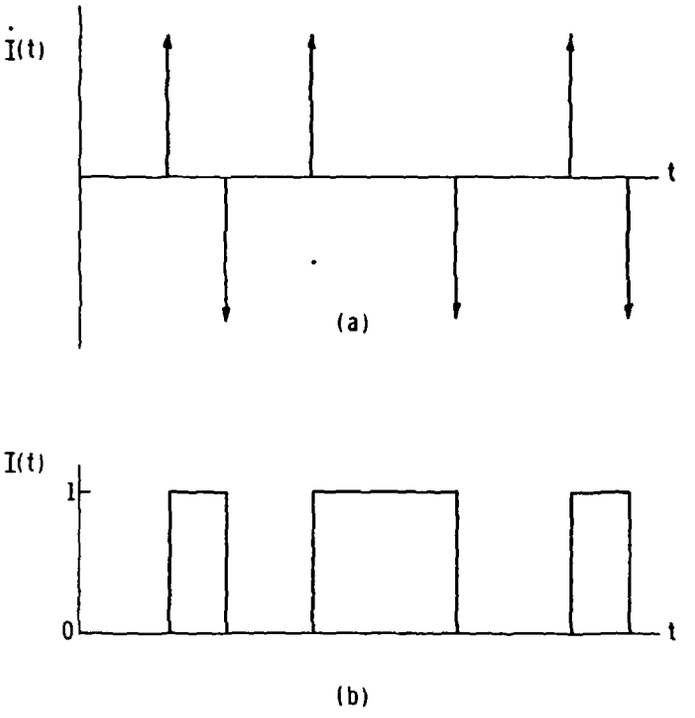

Fig. 3. The idealistic point process (a) and the ideal indicator function (b).

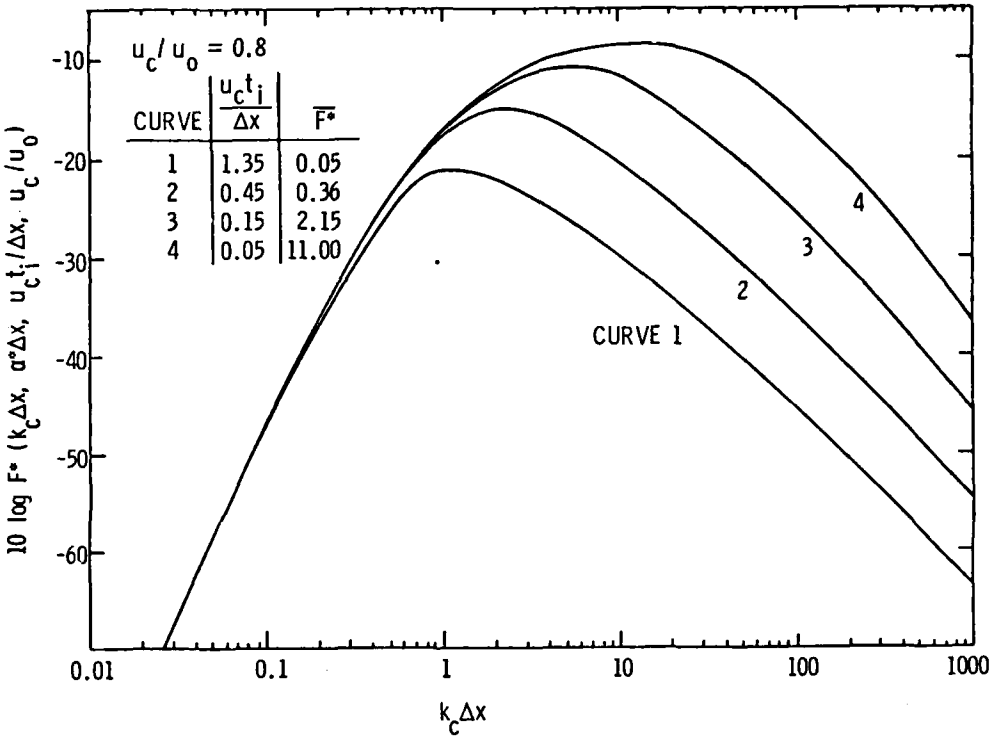

Fig. 4. Non-dimensional power spectral density function of Eq. (23) for $u_c = 0.8\ u_0$.

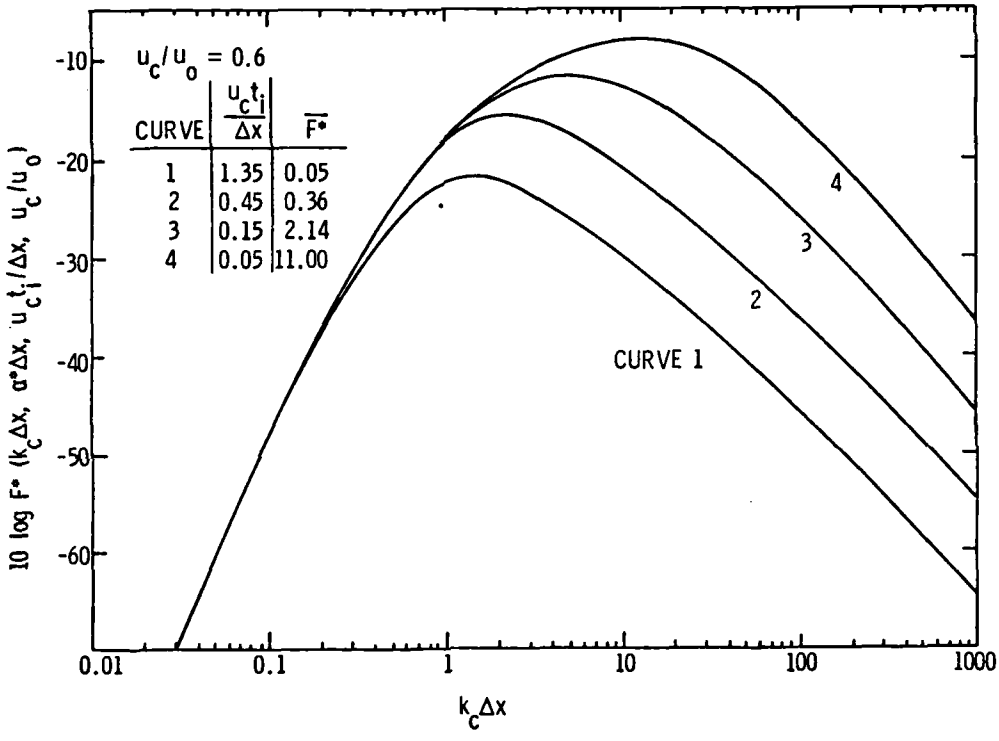

Fig. 5. Non-dimensional power spectral density function of Eq. (23) for $u_c = 0.6\ u_0$.

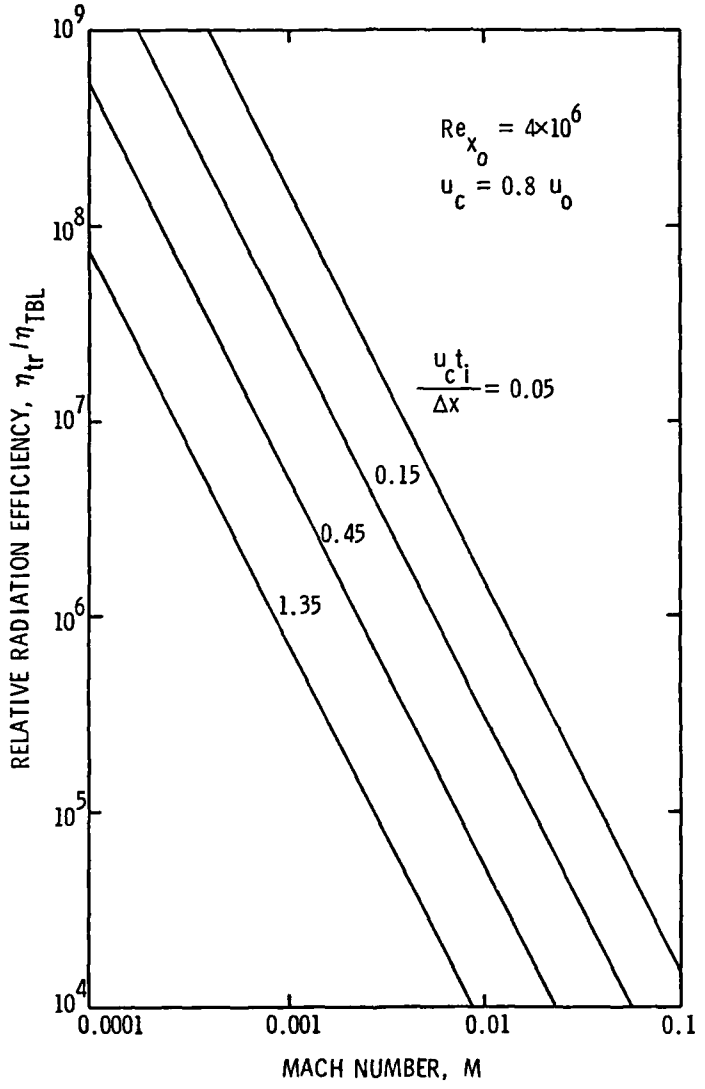

Fig. 6. Relative radiation efficiency, η_{tr}/η_{TBL}, expressed as a function of Mach number.

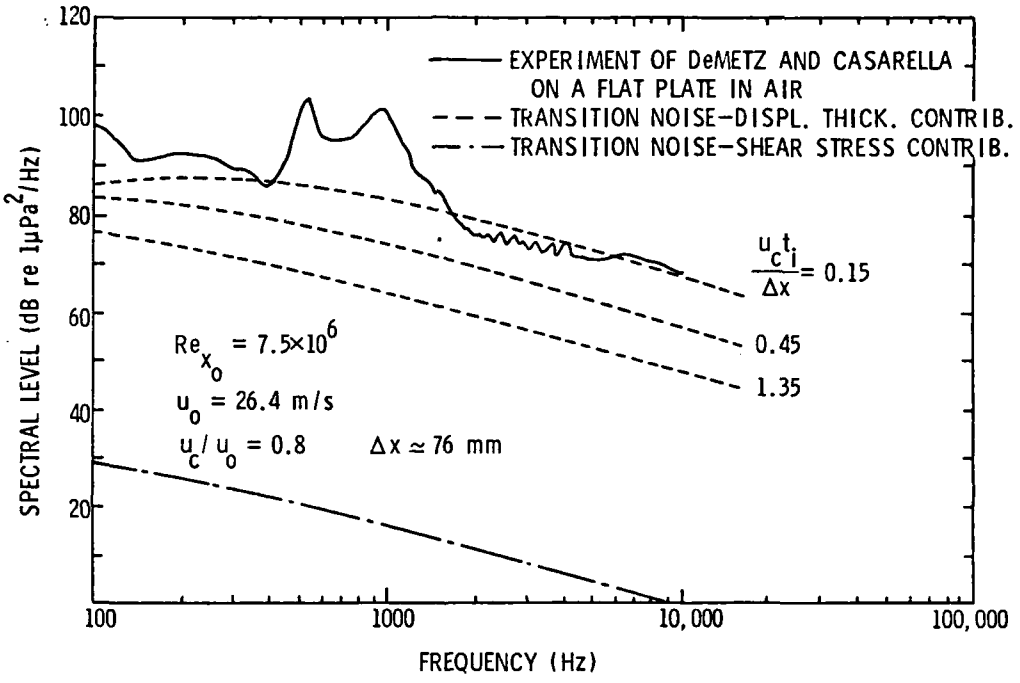

Fig. 7. Comparison of the theory with an experimental spectrum measured on a flat plate by DeMetz and Casarella [13].

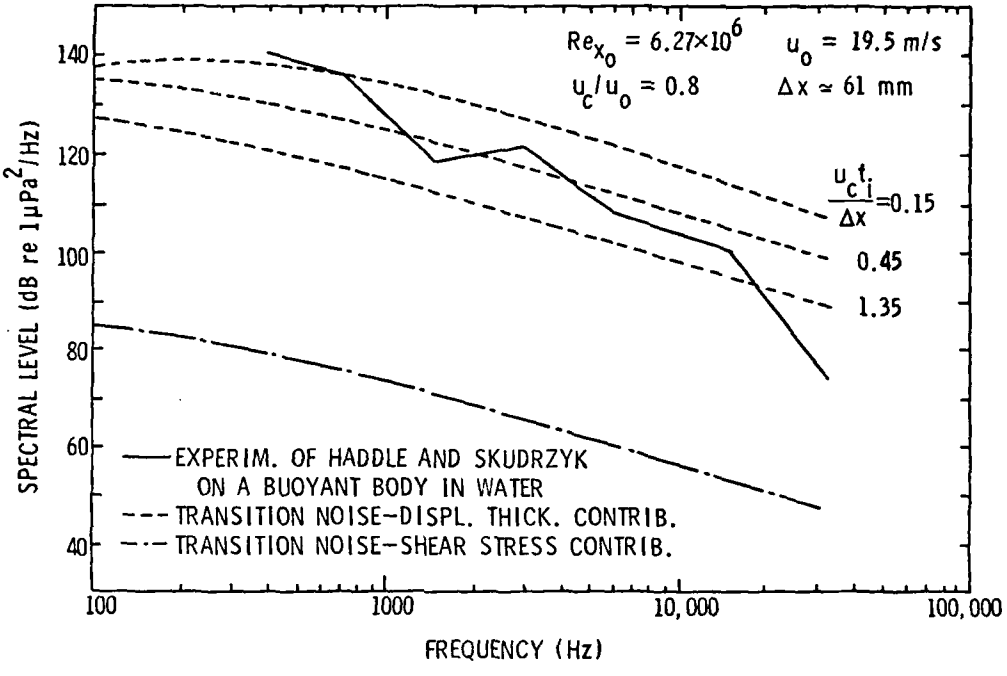

Fig. 8. Comparison of the theory with an experimental spectrum measured on the surface of a buoyantly - propelled vehicle by Haddle and Skudrzyk [2].

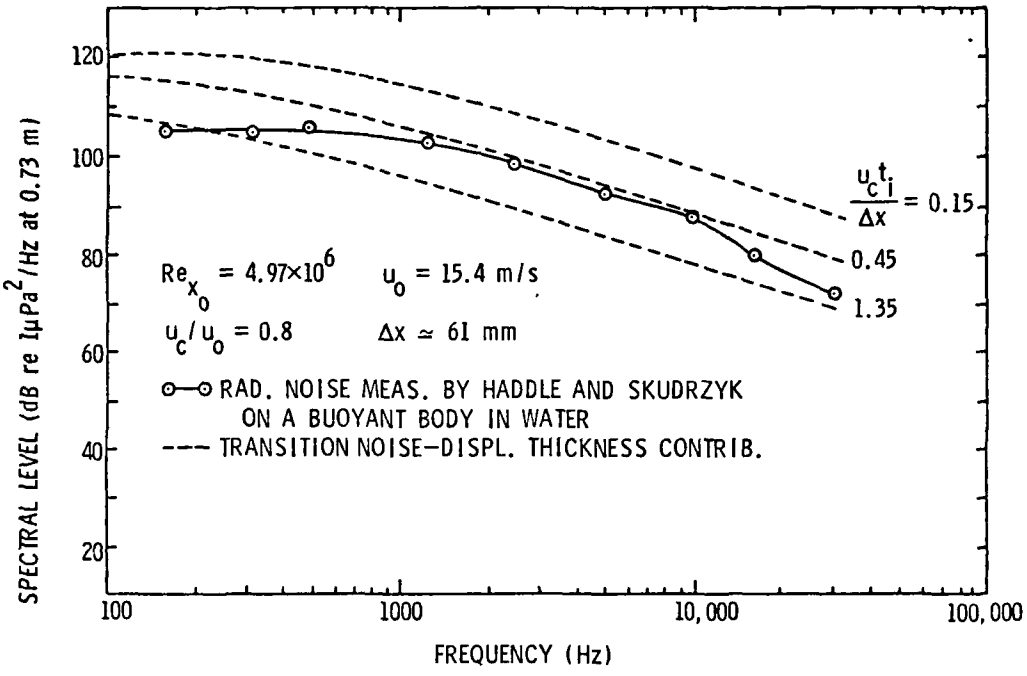

Fig. 9. Comparison of the theory with an experimental spectrum measured far away from the rising buoyant body of Haddle and Skudrzyk [2].

DISTRIBUTION LIST FOR UNCLASSIFIED TM 80-41 by G. C. Lauchle, dated 27 March 1980

Commander
Naval Sea Systems Command
Department of the Navy
Washington, DC 20362
Attn: Library
Code NSEA-09G32
(Copies No. 1 and 2)

Naval Sea Systems Command
Attn: E. G. Liszka
Code NSEA-63R1
(Copy No. 3)

Naval Sea Systems Command
Attn: F. Romano
Code NSEA-63R
(Copy No. 4)

Naval Sea Systems Command
Attn: T. E. Peirce
Code NSEA-63R-31
(Copy No. 5)

Naval Sea Systems Command
Attn: J. G. Juergens
Code NSEA-05H
(Copy No. 6)

Naval Sea Systems Command
Attn: H. C. Claybourne
Code NSEA-05H
(Copy No. 7)

Naval Sea Systems Command
Attn: A. R. Paladino
Code NSEA-05H1
(Copy No. 8)

Naval Sea Systems Command
Attn: C. C. Taylor
Code NSEA-05H
(Copy No. 9)

Naval Sea Systems Command
Attn: D. L. Creed
Code NSEA-00311
(Copy No. 10)

Naval Sea Systems Command
Attn: W. L. Louis
Code NSEA-32132
(Copy No. 11)

Naval Sea Systems Command
Attn: F. J. Welling
Code NSEA-521
(Copy No. 12)

Commanding Officer
Naval Underwater Systems Center
Newport, RI 02840
Attn: C. N. Pryor
Code 01
(Copy No. 13)

Naval Underwater Systems Center
Attn: D. Goodrich
Code 36315
(Copy No. 14)

Naval Underwater Systems Center
Attn: R. J. Kittredge
Code 36313
(Copy No. 15)

Naval Underwater Systems Center
Attn: J. Miguel
Code 36315
(Copy No. 16)

Naval Underwater Systems Center
Attn: B. J. Myers
Code 36311
(Copy No. 17)

Naval Underwater Systems Center
Attn: R. H. Nadolink
Code 36315
(Copy No. 18)

Naval Underwater Systems Center
Attn: D. A. Quadrini
Code 36314
(Copy No. 19)

Naval Underwater Systems Center
Attn: E. J. Sullivan
Code 36311
(Copy No. 20)

Naval Underwater Systems Center
Attn: R. Trainor
Code 36314
(Copy No. 21)

Naval Underwater Systems Center
Attn: Library
Code 54
(Copy No. 22)

Naval Ocean Systems Center
San Diego, CA 92152
Attn: M. M. Reischman
Code 2542
(Copy No. 23)

DISTRIBUTION LIST FOR UNCLASSIFIED TM 80-41 by G. C. Lauchle, dated 27 March 1980

Commander
David W. Taylor Naval Ship R&D Center
Department of the Navy
Bethesda, MD 20084
Attn: Code 1505
(Copy No. 24)

David W. Taylor Naval Ship R&D Center
Attn: J. H. McCarthy
Code 1552
(Copy No. 25)

David W. Taylor Naval Ship R&D Center
Attn: T. E. Brockett
Code 1544
(Copy No. 26)

David W. Taylor Naval Ship R&D Center
Attn: M. M. Sevik
Code 19
(Copy No. 27)

David W. Taylor Naval Ship R&D Center
Attn: W. K. Blake
Code 1942
(Copy No. 28)

David W. Taylor Naval Ship R&D Center
Attn: T. M. Farabee
Code 1942
(Copy No. 29)

David W. Taylor Naval Ship R&D Center
Attn: M. J. Casarella
Code 1942
(Copy No. 30)

Officer-in-Charge
David W. Taylor Naval Ship R&D Center
Department of the Navy
Annapolis Laboratory
Annapolis, MD 21402
Attn: J. G. Stricker
Code 2721
(Copy No. 31)

Commander
Naval Surface Weapon Center
Silver Spring, MD 20910
Attn: G. C. Gaunaurd
Code R-31
(Copy No. 32)

Naval Surface Weapon Center
Attn: Library
(Copy No. 33)

Office of Naval Research
Department of the Navy
800 N. Quincy Street
Arlington, VA 22217
Attn: H. Fitzpatrick
Code 438
(Copy No. 34)

Office of Naval Research
Attn: R. D. Cooper
Code 438
(Copy No. 35)

Naval Research Laboratory
Attn: R. J. Hansen
Code 20375
(Copy No. 36)

Defense Technical Information Center
5010 Duke Street
Cameron Station
Alexandria, VA 22314
(Copies No. 37 - 48)

National Bureau of Standards
Aerodynamics Section
Washington, DC 20234
Attn: P. S. Klebanoff
(Copy No. 49)

Rand Corporation
1700 Main Street
Santa Monica, CA 90406
Attn: C. Gazley
(Copy No. 50)

Jet Propulsion Laboratory
4800 Oak Grove Drive
Pasadena, CA 91108
Attn: L. M. Mack
(Copy No. 51)

Hersh Acoustical Engineering
9545 Cozycroft Avenue
Chatsworth, CA 91311
Attn: A. Hersh
(Copy No. 52)

Dynamics Technology, Inc.
3838 Carson Street, Suite 110
Torrance, CA 90503
Attn: W. N. Haigh
(Copy No. 53)

Dynamics Technology, Inc.
Attn: D. R. S. Ko
(Copy No. 54)

DISTRIBUTION LIST FOR UNCLASSIFIED TM 80-41 by G. C. Lauchle, dated 27 March 1980

Bolt Beranek and Newman
50 Moulton Street
Cambridge, MA 20136
Attn: N. Brown
(Copy No. 55)

Bolt Beranek and Newman
Attn: D. Chase
(Copy No. 56)

Bolt Beranek and Newman
Attn: K. L. Chandiramani
(Copy No. 57)

Kentex International, Inc.
2054 University Avenue - #301
Berkeley, CA 94704
Attn: S. Yang
(Copy No. 58)

Bell Laboratories
Whippany Road
Whippany, NJ 07981
Attn: J. G. Berryman
(Copy No. 59)

Massachusetts Institute of Technology
77 Massachusetts Avenue
Cambridge, MA 02139
Attn: Prof. Patrick Leehey
Department of Ocean Engineering
Room 5-222
(Copy No. 60)

Massachusetts Institute of Technology
Attn: M. T. Landahl
(Copy No. 61)

Cornell University
Sibley School of Mechanical and
Aeronautical Engineering
Upson Hall
Ithaca, NY 14850
Attn: Dr. J. L. Lumley
(Copy No. 62)

University of Minnesota
St. Anthony Falls Hydraulic Laboratory
Mississippi River at 3rd Avenue S.E.
Minneapolis, MN 55414
Attn: R. E. A. Arndt
(Copy No. 63)

University of Minnesota
Attn: L. G. Straub Memorial Library
(Copy No. 64)

University of Leeds
Department of Applied Mathematical Studies
Leeds LS29JT, England
Attn: Dr. D. G. Crighton
(Copy No. 65)

A. G. Fabula
5497 Coral Reef Avenue
La Jolla, CA 92037
(Copy No. 66)

O. F. Griffith
Department of Physics
University of New Orleans
Lake Front
New Orleans, LA 70122
(Copy No. 67)

Mark V. Morkovin
Department of Mech. and Aerosp. Engr.
Illinois Inst. of Tech.
3300 S. Federal Street
Chicago, Illinois 60616
(Copy No. 68)

William K. George
SUNY at Buffalo
Department of Mechanical Engineering
Parker Engr. Building
Buffalo, NY 14214
(Copy No. 69)

L. Maestrello
MS 460
NASA Langley Research Center
Hampton, VA 23665
(Copy No. 70)

R. F. Mons
Westinghouse Electric Corp.
P.O. Box 1458
Annapolis, MD 21404
(Copy No. 71)

Applied Research Laboratory
The Pennsylvania State University
Post Office Box 30
State College, PA 16801
Attn: B. R. Parkin
(Copy No. 72)

Applied Research Laboratory
Attn: E. J. Skudrzyk
(Copy No. 73)

DISTRIBUTION LIST FOR UNCLASSIFIED TM 80-41 by G. C. Lauchle, dated 27 March 1980

Applied Research Laboratory
Attn: G. H. Hoffman
(Copy No. 74)

Applied Research Laboratory
Attn: G. C. Lauchle
(Copy No. 75)

Applied Research Laboratory
Attn: GTWT File
(Copy No. 76)